

Effects of Particle Size on Photoassisted Water–Gas Shift Reaction over Pt/TiO₂

Recently, we have studied the photoassisted water-gas shift reaction over a small-area single crystal TiO₂ (100) with different Pt coverages (1). Based on these results, we proposed a reaction mechanism assuming CO photoreduction of TiO₂ at Pt–TiO₂ periphery sites to be the rate-limiting step. The steady state reaction probability at optimum Pt coverage (about 0.6 monolayer) was found to be 1×10^{-5} hydrogen molecule/photon in the range 3.0–3.9 eV. This low reaction probability can be attributed to the small area of the photocatalyst we used and the inefficient collection of photo-generated charge carriers deep beneath the TiO₂ surface. Clearly, platinized TiO₂ powder catalysts should have higher activity because of the larger total number of active sites. Moreover, when the TiO₂ particle size is less than the (minority) carrier diffusion length, charge carriers photogenerated inside the particle can diffuse to the surface and contribute to the photoreaction, thereby achieving a higher reaction probability (1). To explore these points, we studied and compared the photoassisted water-gas shift reaction rates over Pt/TiO₂ powders with different TiO₂ particle sizes.

Titanium dioxide (anatase) powders with two different average particle sizes were used. TiO₂(A) has an average particle radius of 800 Å. TiO₂(B), obtained from Degussa Company and commonly known as P25, has an average particle radius of 150 Å. Before Pt impregnation, TiO₂ powders were reduced in flowing H₂ at 600°C for 3 h. The sample was then cooled to room temperature in flowing H₂ before being removed from the furnace. Scanning electron microscopy observations of TiO₂(A)

showed no significant sintering after such treatments. Platinum was photodeposited onto the TiO₂ surface according to the method described by Kraeutler and Bard (2). The Pt loading was determined using weight gain and Auger analysis. In the Auger method, a calibration curve of Pt(65 eV)/Ti(380 eV) ratio versus Pt coverage was first generated. The calibration was performed by depositing Pt onto a TiO₂(100) single crystal. The Pt(65 eV)/Ti(380 eV) ratio was measured. The associated amount of Pt deposited was determined by the attenuation of O(510 eV) Auger peak, assuming an electron mean free path of 10 Å. Then platinized TiO₂ powders were sprinkled onto an indium foil and loaded into a Physical Electronics 590A scanning Auger microprobe to determine the Pt(65 eV)/Ti(380 eV) ratio for the catalyst. From this and the calibration curve, the Pt coverage was determined. These results are presented in Table 1.

It should be noted that these two methods (weight gain and Auger analysis) of Pt coverage measurements are consistent. For instance, in the case of TiO₂(B) powder with an average radius of 150 Å, an average Pt coverage of 1 Å corresponds to a weight gain of 11%. The measured 5% weight gain translates to 0.45 Å Pt coverage, which is in close agreement with Auger results (0.5 ± 0.1 Å).

Platinized TiO₂ powders with a weight of 150 mg were compressed into a disk of diameter of 0.5 in. It was mounted on a gold foil holder. Temperature measurement was furnished by a thermocouple in contact with the disk surface. The whole unit was then mounted on a reaction cell which has

TABLE 1
Platinum Coverages on Pt/TiO₂(A) and Pt/TiO₂(B)
Powders

Sample	Average TiO ₂ particle radius (Å)	Pt (weight%)	Pt thickness by Auger analysis (Å)
Pt/TiO ₂ (A)	800	1.0 ± 0.2	(0.5 ± 0.1)
Pt/TiO ₂ (B)	150	5.0 ± 0.2	(0.5 ± 0.1)

been described in detail elsewhere (1). Briefly, it is a stainless-steel six-way cross-reaction chamber attached to a UHV chamber through a gate valve. The UHV chamber maintains a base pressure of 2×10^{-9} Torr. The specimen was mounted on one end of a transfer tube inside the reaction cell. Before reaction, the sample was reduced in 2 Torr H₂ at 250°C for 2 h in the reaction cell, followed by outgassing under UHV at 350°C for 3 h. After specimen cool-down to near room temperature, the gate valve between the UHV chamber and the reaction cell was closed. Water vapor (18 Torr) and CO (0.3 Torr) were introduced into the reaction cell. The cell was finally pressurized with argon to a total pressure of 50 Torr to ensure proper gas sampling for gas chromatography analysis. Ultraviolet illumination was provided by a high-pressure mercury arc lamp operating at 250 W with its output filtered through a NiSO₄ solution (200 g/liter) to remove the infrared. The photon output between 3.0 and 3.9 eV is 10 mW. During the reaction, the gas products were analyzed by a thermal conductivity gas chromatograph.

Major products of the photoreaction were hydrogen and carbon dioxide. Trace amount of methane was also observed. The CO₂/H₂ ratio was close to unity, indicating that the water-gas shift reaction was the major reaction. Figure 1 shows a typical time course of the production of hydrogen from the photoassisted water-gas shift reaction at 60°C. Apart from an initial transient, the reaction maintained a rather constant rate. This steady state rate was maintained

even after the cell was evacuated and new reactant gases were introduced.

The steady state hydrogen production rate was measured for Pt/TiO₂(A) and Pt/TiO₂(B), and the results are given in Table 2. Reaction rates shown in Table 2 are net reaction rates after subtracting the thermal reaction contribution. The thermal reaction was performed by heating the specimen using a heating lamp under otherwise identical experimental conditions. The radiation from the heating lamp was filtered to cut off the uv.

Although 150 mg of Pt/TiO₂ powders was used in our experiment, only a small portion of it was expected to be exposed to uv due to the limited uv penetration depth. The rest of the sample can only contribute to the reaction through the thermal reaction channel. In our experiment, the most intense uv radiation with energy between 3.0 and 3.9 eV peaks at 3.3 eV. According to Eagles (3), the penetration of 3.3-eV photons in TiO₂ is about 3300 Å. Using this penetration depth, one can show that the effective surface area for the Pt/TiO₂(A) and Pt/TiO₂(B) disk is 15.8 and 83.6 cm², respectively. Reaction rates per unit area were calculated and shown in Table 2. It can be seen from these results that the pho-

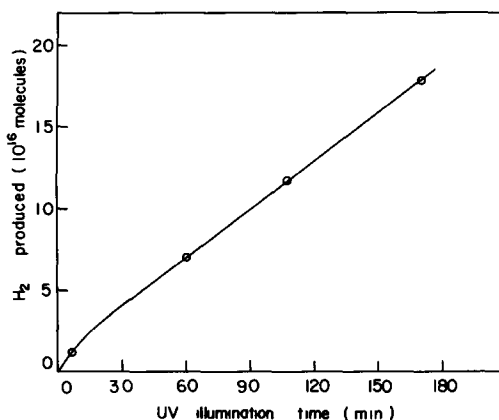


FIG. 1 The number of hydrogen molecules produced from uv-irradiated Pt/TiO₂(A) powders (weight 150 mg) at 60°C as a function of reaction time with $P_{\text{H}_2} = 18$ Torr and $P_{\text{CO}} = 0.3$ Torr.

TABLE 2
Photoassisted Water-Gas Shift Reaction Rate from
Different Pt/TiO₂ Photocatalysts

Sample	Pt/TiO ₂ (A)	Pt/TiO ₂ (B)	Pt/TiO ₂ (100) ^a
Photoreaction rate at 60°C (0.5 Å Pt coverage) in 10 ¹⁵ H ₂ /h	50	1240	0.13
Effective surface area for photoreaction (cm ²)	15.7	83.6	0.63
Photoreaction rate at 60°C (0.5 Å Pt coverage) in 10 ¹⁵ H ₂ /h cm ²	3.18	14.8	0.2

Note: Reactions were performed at 18 Torr of water vapor and 0.3 Torr of CO

^a From Ref. (1)

photoreaction rate per unit area R depends on particle size (or average radius r). In Fig. 2, R is plotted as a function of $1/r$, showing that R appears to be proportional to $1/r$. It should be admitted, however, that this linear dependence on $1/r$ is not completely convincing due to the limited number of data points. But it is very clear that the reaction rate per unit area does depend on the particle size and increases with decreasing particle size. It should be emphasized here that this particle size dependence still holds even if the value we assumed for the uv penetration depth is incorrect. By using a different penetration depth, all the photoreaction effective surface areas and hence specific reaction rates will differ by an identical scaling factor. This would only change the vertical scale of Fig. 2.

In our previous study using single crystal Pt/TiO₂ (100), we always observed an initial transient in the photoproduction of the first monolayer of hydrogen (1). This is no exception in the present experiment. For example, Fig. 1 shows an initial transient in the production of the first $1-2 \times 10^{16}$ molecules of H₂ from Pt/TiO₂(A). This is consistent with our estimate of 15.7 cm² for the effective surface area of Pt/TiO₂(A) and justifies this use of effective area for obtaining specific activities.

Sato and White (4) performed similar experiments on powdered 2 wt% Pt/TiO₂ us-

ing a Hg arc lamp operating at 200 W. The Pt/TiO₂ powders were spread uniformly over the bottom of a 180-ml flask, the area of which we guessed to be roughly 50 cm². At 60°C and similar reactant conditions, the total hydrogen photoproduction rate reported by Sato and White (4) translated to 4.4×10^{18} molecules/h. The average TiO₂ particle radius was 710 Å. Using a uv penetration depth of 3300 Å, the total effective surface area is about 700 cm². This amounts to about 6.3×10^{15} molecules/h-cm² at 200 W or 7.8×10^{15} /h-cm² at 250 W, assuming linear dependence on uv intensity (1, 4). One wt% Pt/TiO₂ is expected to have a hydrogen photoproduction rate roughly half that of the 2 wt% photocatalyst (Fig. 3, Ref. (1)), i.e., 3.9×10^{15} /h-cm². This compares favorably with the corresponding value for our 1 wt% Pt/TiO₂(A) (particle radius 800 Å) of 3.2×10^{15} /h-cm².

It should be mentioned that we did not know whether or not the TiO₂(B) powders underwent sintering during the reduction treatment. The consistency between weight gain and Auger results suggests that significant sintering did not take place. If sintering did take place for TiO₂(B), the true specific activity would have been even higher.

Based on a model proposed previously for the photoassisted water-gas shift reaction (1), the rate-determining step is CO

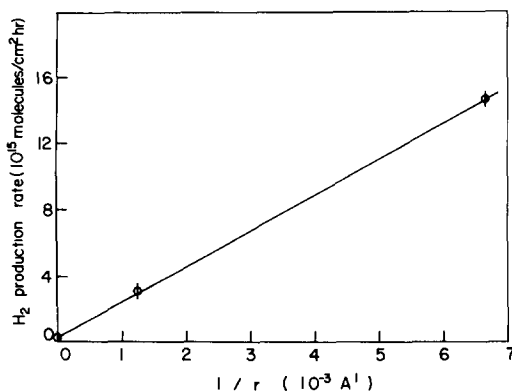


FIG. 2 The relationship between hydrogen production rate per unit area R from Pt/TiO₂ photocatalysts and the average radius of catalysts.

photoreduction of TiO_2 at Pt- TiO_2 periphery sites and the reaction rate per unit area R is given by

$$R = kpl \quad (1)$$

where k is a constant, p the surface hole concentration, and l the Pt island perimeter per unit area. Studies by Ghosh and Maruska (5) showed that the hole diffusion length L is $1.2 \mu\text{m}$ for TiO_2 . With this L value, the $L \gg r$ (r being TiO_2 particle radius) condition is fairly well satisfied for our two samples. Therefore, for particles within the uv penetration depth, all holes photogenerated within them can diffuse to the surface and may then be utilized. In other words, p is proportional to total uv absorption volume/area, i.e., $p \propto r$ for our two photocatalysts. Since R is observed to be proportional to $1/r$, this implies that l is proportional to $1/r^2$. This dependence suggests that there are morphological (6, 7) or compositional changes (8) as the titania particle size decreases. In the latter case, there is evidence in related system (8-10) that extensive interdiffusion between the metal and titania can occur during reduction treatment of the catalyst.

ACKNOWLEDGMENTS

This work is supported by the Department of Energy, Division of Material Sciences under Grant DE-AC02-78ER4946.

REFERENCES

- 1 Tsai, S. C., Kao, C. C., and Chung, Y. W., *J. Catal.* **79**, 451 (1983).
- 2 Kraeutler, B., and Bard, A. J., *Amer. Chem. Soc.* **100**, 4317 (1978).
- 3 Eagles, Jr., D. M., *Phys. Chem. Solids* **25**, 1243 (1964).
- 4 Sato, S., and White, J. M., *J. Amer. Chem. Soc.* **102**, 7206 (1980).
- 5 Ghosh, A. K., and Maruska, H. P., *J. Electrochem. Soc.* **124**, 1516 (1977).
- 6 Blakely, D. W., and Somorjai, G. A., *J. Catal.* **42**, 181 (1976).
- 7 Van Hardeveld, R., and Hartog, F., *Surf. Sci.* **15**, 189 (1969).
- 8 Santos, J., Phillips, J., and Dumesic, J. A., *J. Catal.* **81**, 147 (1983).
- 9 Resasco, D. E., and Haller, G. L., *J. Catal.* **82**, 279 (1983).
- 10 Kao, C. C., Tsai, S. C., Bahl, M. K., Chung, Y. W., and Lo, W. J., *Surf. Sci.* **95**, 1 (1980).

SHOU-CHIN TSAI

*Texas Instruments
Dallas, Texas 75222*

YIP-WAH CHUNG

*Department of Materials
Science and Engineering
Northwestern University
Evanston, Illinois 60201*

Received August 18, 1983